Characterization of novel murine anti-CD20 monoclonal antibodies and their comparison to 2B8 and c2B8 (rituximab)

MICHIO NISHIDA[1], SADAKAZU USUDA[2], MASATO OKABE[2,3], HIROKO MIYAKODA[3], MIDORI KOMATSU[4], HIROSHI HANAOKA[5], KEISUKE TESHIGAWARA[1] and OTSURA NIWA[1]

[1]Late Effects Studies, Radiation Biology Center, Kyoto University, Yoshida-Konoe-cho, Sakyo-ku, Kyoto 606-8501; [2]BioMedics Japan, Inc, 1-1-10 Koraku, Bunkyo, Tokyo 112-0004; [3]Bacteriology Division, Faculty of Medicine, Tottori University, 86 Nishi-machi, Yonago 683-8503; [4]Digestive Surgery, Osaka City University Graduate School of Medicine, 1-4-3 Asahi-cho, Abeno-ku, Osaka 545-8586; [5]Bioimaging Information Analysis, Gunma University, Graduate School of Medicine, 3-39-22 Showa-cho, Maebashi 371-8511, Japan

Received March 2, 2007; Accepted April 27, 2007

Abstract. Rituximab is the first anti-cancer antibody approved by the FDA for the treatment of B-cell non-Hodgkin lymphoma (B-NHL), alone or in combination with chemotherapeutic drugs. Further, rituximab is now being examined in a variety of CD20$^+$ neoplastic diseases as well as B-cell-induced autoimmune diseases. The clinical response to rituximab is significant, resulting not only in tumor regression but also prolongation of survival. However, a subset of patients does not initially respond to rituximab or develops resistance to its further treatment. Therefore, alternative therapies for these patients are strongly desired. Rituximab activity has been thought to be by antibody-dependent cellular cytotoxicity, complement-dependent cytotoxicity and apoptosis, and studies in model systems established the role of rituximab in cell signaling-induced perturbation of anti-apoptotic survival pathways, suggesting that the patients unresponsive to rituximab may be overcome with other CD20 antibodies with different activities. This study investigated eight novel murine antibodies directed against CD20 for their physical and biological properties in comparison with 2B8 and c2B8 (rituximab). These antibodies were derived by various antigenic and immunization procedures and selected for CD20 activity. Analysis of these antibodies revealed that they all bound to various B-cell lines and CD20-transfected CHO cells. Six of the eight antibodies shared similar variable-region amino acid sequences that were also shared by 2B8 while two monoclonal antibodies did not. Of them, 1K1791 has a distinct heavy chain and both 1K1791 and 1K1782 have distinct light chains. Not all of the antibodies inhibited cell growth and only two antibodies reacted with fixed GST-CD20 recombinant fusion protein. Noteworthy, 1K1791 was found to inhibit cell proliferation and also induced caspase-independent apoptosis in the absence of cross-linker. These findings identified new antibodies with properties and epitope specificities different from 2B8. The potential clinical application of such antibodies in the treatment of B-NHL and rituximab-resistant B-NHL is discussed.

Correspondence to: Michio Nishida, Late Effects Studies, Radiation Biology Center, Kyoto University, Yoshida-Konoe-cho, Sakyo-ku, Kyoto 606-8501, Japan
E-mail: minishida@aol.com

Key words: anti-CD20 monoclonal antibody, apoptosis, caspase, epitope specificity

Introduction

Since the introduction of the first monoclonal antibody (mAb), rituximab, for the treatment of B-cell non-Hodgkin lymphoma (B-NHL), several monoclonal antibodies have been approved for many neoplastic and non-neoplastic diseases (1,2). However, while such antibodies show therapeutic effectiveness, their mechanism of action *in vivo* remains elusive. Further, it is not known what are the best regimens and schedules under which such antibodies are best suited for a particular patient. In addition, treatment with such antibodies results only in a subset of patients responding and some patients who initially respond also develop resistance to further treatment. Therefore, there is a need to unravel the *in vivo* mechanisms of action as well as develop new classes of antibodies with different activities and clinical responses.

The CD20 molecule is a member of the MS4A family of proteins. It spans the plasma membrane four times and both C- and N-termini are contained within the cell (3-6). The precise function of CD20 is unknown and it has been reported to act as an ion channel expressed in the plasma membrane of normal and malignant B cells. Liang *et al* have reported that CD20 may operate as a calcium storage channel facilitating entry of intracellular calcium following BCR-induced emptying of intracellular calcium (4). The importance of CD20 as a target for mAb immunotherapy is irrefutable, and anti-CD20 monoclonal antibodies appear to be ideal for B-cell diseases. It is highly expressed on the plasma membrane of almost all plasma B cells but not on hematological stem cells; it is not shed from the surface after antibody binding and is not shed into the circulation (5).

It has been reported that rituximab can mediate antibody-dependent cellular cytotoxicity (ADCC), complement-dependent cytotoxicity (CDC) and apoptosis both *in vitro* and *in vivo*, and the target epitope is critical in determining which of these various mechanisms predominates (7,8). In the case of anti-CD20, evidence suggests that Fc/Fc-receptor (FcR) interactions are critical, as determined in both animal models and humans. However, determining whether such interactions are required for classical ADCC-mediated by NK or myeloid cells or whether they provide cross-linking which promotes apoptosis has been difficult to resolve (9,10). The role of complement in the depletion of malignant cells is less convincing, and a number of anti-tumor mAbs appear to operate in the absence of lytic complement (11-13). A strong correlation between the level of CD20 expression and therapeutic outcome for rituximab has been reported, although there is also contrary evidence where no correlation was found (14,15). Chan *et al* have reported a CD20 mAb which is potent in CDC and less effective in apoptosis, whereas a different antibody was ineffective in CDC with potent induction of apoptosis (16). Both were equally effective in ADCC. Rituximab is currently being used in the management of NHL patients as a single agent or in combination with CHOP. It also shows clinical response in patients with chronic lymphocytic leukemia (17). Rituximab is also used in autoimmune disease such as rheumatoid arthritis and has recently been approved for treatment of patients with moderate to advanced rheumatoid disease (18).

Following binding of anti-CD20 mAb to cells recruitment of effector cells for ADCC (antibody-dependent cellular cytotoxicity) and CDC (complement-dependent cytotoxicity) occurs. In addition, when CD20 is engaged by mAb, it can trigger transmembrane signaling directly and inhibit cell growth and trigger cell death in certain tumors. Further, it has also been shown to sensitize tumor cells to both chemotherapy and immunotherapy (6). Different anti-CD20 mAbs have been shown to have different properties and epitope specificities, and mediate differential effects on CDC and cell death. All of the monoclonal antibodies described to date recognize the extracellular loop and partially or completely cross-block each other's binding (19-21).

In the current study, we have developed a number of murine anti-CD20 mAbs and compared their activities to the published antibodies 1F5, 2B8 and c2B8. We have identified new mAbs with different activities and binding specificities.

Materials and methods

Cells and antibodies. The $CD20^+$ cell lines, Raji (Burkitt's lymphoma), CCRF-SB (acute lymphoblastic leukemia) and the $CD20^-$ cell line Jurkat (T cell leukemia), were obtained from the Riken Bioresource Center, Japanese Collection of Research Bioresources (JCRB; Tsukuba, Japan) and the American Type Culture Collection (ATCC; Manassas, VA). CHO DG44 was obtained from Invitrogen Japan (Tokyo, Japan) (22). The full CD20 DNA-transfected CHO cell line ($CD20^+$ CHO) was collaboratively developed by Tottori University (Yonago, Japan) and BioMedics Japan, Inc. (Tokyo, Japan).

The murine 1K mAbs (Table I) specifically binding to human CD20 were provided by BioMedics Japan. BALB/c mice (purchased from CLEA Japan, Tokyo, Japan) were immunized with various combinations of Raji cells, CCRF-SB cells, recombinant fusion protein of CD20 extracellular domain with glutathione S-transferase (GST) and CD20 DNA transfected CHO cells (23).

The murine anti-CD20 mAb 2B8 and the chimeric anti-CD20 mAb c2B8 (rituximab) were obtained from Zenyaku Kogyo (Tokyo, Japan). The murine anti-CD20 antibody 1F5, normal murine IgG1, IgG2a and IgG2b were purchased from Dako Japan (Kyoto, Japan), and murine anti-human CD3 mAb was from BD Biosciences (San Jose, CA).

Flow cytometry. Various mAbs and control immunoglobulin (Ig) isotypes were used to determine their binding properties on the cell surface of $CD20^+$ cell lines or $CD20^-$ cells. The cells ($2x10^6$ cells) were suspended in RPMI-1640 culture medium (Sigma Chemical, St Louis, MO) containing 10% fetal bovine serum (FBS) (ICN Biochemicals, Costa Mesa, CA) and were centrifuged at 1300 x rpm for 3 min. The supernatants were discarded and the pellets resuspended in 550 μl phosphate buffered saline (PBS) containing 4% FBS. Aliquots of 50 μl PBS containing 4% FBS each were placed in Eppendorf tubes and 5 μl (10 μg/ml) of each antibody or control IgG were added to the tube and incubated for 30 min at 4˚C. The tubes were centrifuged and the pellets washed twice and then resuspended into 50 μl PBS containing 4% FBS and 5 μl FITC-conjugated $F(ab')_2$ goat anti-mouse Ig (Dako, Japan). The tubes were left for 20 min at 4˚C, washed twice and the pellets were resuspended in 12x75-mm tubes (BD Falcon, BD Biosciences). The flow data were then analyzed by FACS Calibur and by the Cell Quest software (BD Biosciences).

Inhibition of cell growth. Raji cells ($5x10^4$ cells/ml) in RPMI-1640 serum-free medium were assessed for cell growth inhibition in the presence of various antibodies or control IgGs. The cells ($5x10^3$ cells/well) were added into 96-well plates and cultured at 37˚C in a 5% CO_2 incubator for 24 h. Thereafter different concentrations of antibody (0.01-1.0 μg/ml) were added and incubated for 24-72 h. At the indicated times of incubation, 10 μl/well of luminescent reagent (Cell Count Kit-8, Dojundo Laboratories, Kumamoto, Japan) was added into each well and incubated for an additional 4 h. The plates were then read in a microplate reader (Hitachi High-Technologies, Tokyo, Japan) and the absorbance at 492 nm was recorded. The percent of cell growth in the presence of each antibody (0.01-1.0 μg/ml) compared to control IgGs and % inhibition were determined.

Affinity measurement by Scatchard analysis. Radiolabeling of antibodies by direct radio-iodination was performed after the chloramine T method (24). 2 μl of Na ^{125}I (740 kBq) was added to 100-μl aliquots of antibody (0.1 mg/ml) in 0.3 M phosphate buffer (pH 7.4) and chloramine T (1 μg in 3 μl), freshly prepared in the same buffer, was added thereafter. After incubation of the mixture for 5 min at room temperature, ^{125}I labeled antibody was purified by the Bio-Spin 6 column (Wako Pure Chemical, Osaka, Japan).

Binding affinity was determined as follows. Buffer solution (100 μl) was added to $1x10^6$ Raji cells and then mixed together. Each 100 μl of ^{125}I labeled antibody solution (containing

Table I. Properties of monoclonal antibodies used in this study.

mAb[a]	Isotype	K_d	B_{max}	Immunization	Source
1K0924	IgG2b, κ	2.23 nM	$0.7x10^6$	CCRF-SB and GST-CD20	BioMedics Japan
1K1228	IgG1, κ	1.26 nM	$1.6x10^6$	CD20+CHO and GST-CD20	BioMedics Japan
1K1402	IgG1, κ	1.25 nM	$1.7x10^6$	CCRF-SB and $CD20^+$ CHO	BioMedics Japan
1K1422	IgG1, κ	2.07 nM	$1.3x10^6$	CCRF-SB and $CD20^+$ CHO	BioMedics Japan
1K1712	IgG2a, κ	1.70 nM	$0.7x10^6$	$CD20^+$ CHO and Raji	BioMedics Japan
1K1736	IgG2b, κ	1.24 nM	$1.7x10^6$	$CD20^+$ CHO and Raji	BioMedics Japan
1K1782	IgG1, κ	NT	NT	$CD20^+$ CHO and Raji	BioMedics Japan
1K1791	IgG1, κ	3.61 nM	$1.5x10^6$	$CD20^+$ CHO and Raji	BioMedics Japan
1F5	IgG2a, κ	1.41 nM	$0.8x10^6$	NA	ATCC
2B8	IgG1, κ	NT	NT	CCRF-SB	Zenyaku Kogyo
c2B8 (rituximab)	IgG1, κ	1.26 nM	$1.3x10^6$	Chimerized mAb of 2B8	Zenyaku Kogyo

NT, not tested; NA, information not available. [a]1K series of monoclonal antibodies were newly developed by BioMedics Japan. 2B8 and c2B8 that were developed by IDEC Pharmaceuticals (San Diego, CA) were obtained through Zenyaku Kogyo.

0.01 μg antibody) and different quantities of non-labeled antibody, 0.01, 0.03, 0.1, 0.3, 1.0, 3 or 10 μg, were added to 100 μl Raji cell suspension and then reacted for 1 h at room temperature. The supernatant from the cell suspension was removed after centrifugation at 1300 rpm for 3 min, and the radioactivity of the cell fraction was measured. The radioactivity of ^{125}I-labeled antibody bound to cells was counted and compared to the initial radioactivity. The binding constants, either Kd (dissociation constant) or Ka (association constant), were determined by Scatchard analysis by plotting specific bound/free ratio (Y axis) vs. bound antibody concentration (X axis). Simultaneously, B_{max} (receptor density) was determined by fitting to the total binding at the saturated concentration of non-labeled antibody.

ELISA with GST-CD20. Glutathione S-transferase (GST) fused with the extracellular domain of CD20 was obtained from the Biochemistry Division, Faculty of Medicine, Tottori University (Yonago, Japan). This fusion protein was solubilized using 6 M sodium hydroxide solution and immobilized on a 96-well PLL plate and washed with a solution containing 150 mM NaCl, 0.5% Tween-20 and 0.1% NaN_3. Blocking treatment was applied at 37˚C for 4 h using the dilution buffer containing 0.2% gelatin, 0.5% bovine serum albumin (BSA) and 0.01% thimerosal. Antibody sample [100 μl (1000, 316, 100, 32, 10 or 3 ng/ml)] was added to the wells and left to react at 37˚C for 4 h (1st reaction). 2B8 was used as a positive control and solution without antibody was used as a negative control. The plate was washed and then 100 μl solution (diluted to 1:4000) of horseradish peroxidase (HRP)-labeled rabbit anti-mouse IgG (Jackson Lab, ME) was added to each well, and incubated at 37˚C for 1 h (2nd reaction). The plate was washed again and 100 μl luminescent liquid was added to each well and the reaction stopped after 30 min by adding 50 μl of 4N H_2SO_4. The plates were read for the absorbance at 492 nm.

Competitive binding assay using the $CD20^+$ CHO ELISA. Of $CD20^+$ CHO cells, 100 μl ($5x10^5$ cells/ml) were added to each well on 96-well PLL plates and immobilized. Blocking treatment was performed at 37˚C for 1 h. Rituximab solution (40 and 80 ng/ml) and 2.0, 0.4 and 0.08 μg/ml of diluted test antibodies as well as 2B8 were prepared. Each combination of diluted rituximab and test antibody was added with $CD20^+$ CHO cells on a cell ELISA plate. The first set of reactions used 60 μl/well of antibody at 37˚C for 4 h and the second set of reactions used diluted solution (x2000) of HRP-labeled anti-human IgG (Jackson Lab) at 37˚C for 1 h, respectively. The color reaction was developed for 20 min at 25˚C under dark and static conditions. H_2O_2 + OPD (100 μl/well) was used for the luminescent liquid and 50 μl/well of 4N H_2SO_4 for the stop solution, and then the absorbance at 492 nm was measured.

Phylogenetic tree analysis of anti-CD20 mAb variable-region amino acid sequences. The relative differences of amino acid sequences of variable regions between a number of anti-CD20 mAbs and 2B8 were mapped and displayed by applying a neighboring-joining method on phylogenetic trees (25). Heavy and light chain variable-region sequences of anti-CD20 mAbs were obtained from several information sources. Those of 2B8, 2H7 and 1F5 were obtained from GenBank (National Center for Biotechnology Information, USA), 9C10, 12E11 and 1K mAbs were derived from BioMedics Japan. These data were analyzed by a computer at the National Institute of Genetics (Mishima, Japan).

Cell death and apoptosis. Apoptosis and necrosis induced by the various mAbs were measured by flow cytometry with Annexin V/FITC, PI (propidium iodine) staining (Annexin V/FITC apoptosis detection kit, BD Biosciences). 2B8 was used as positive control and murine anti-CD3 mAb (BioLegend, San Diego, CA) as the negative control (note: the amount of 1K1782 was not enough to complete the study).

Analysis of caspase activation. For titrating rituximab, 100 μl of RPMI-1640 medium containing 10% heat-inactivated FBS and penicillin/streptomycin (Invitrogen, Carlsbad, CA) were

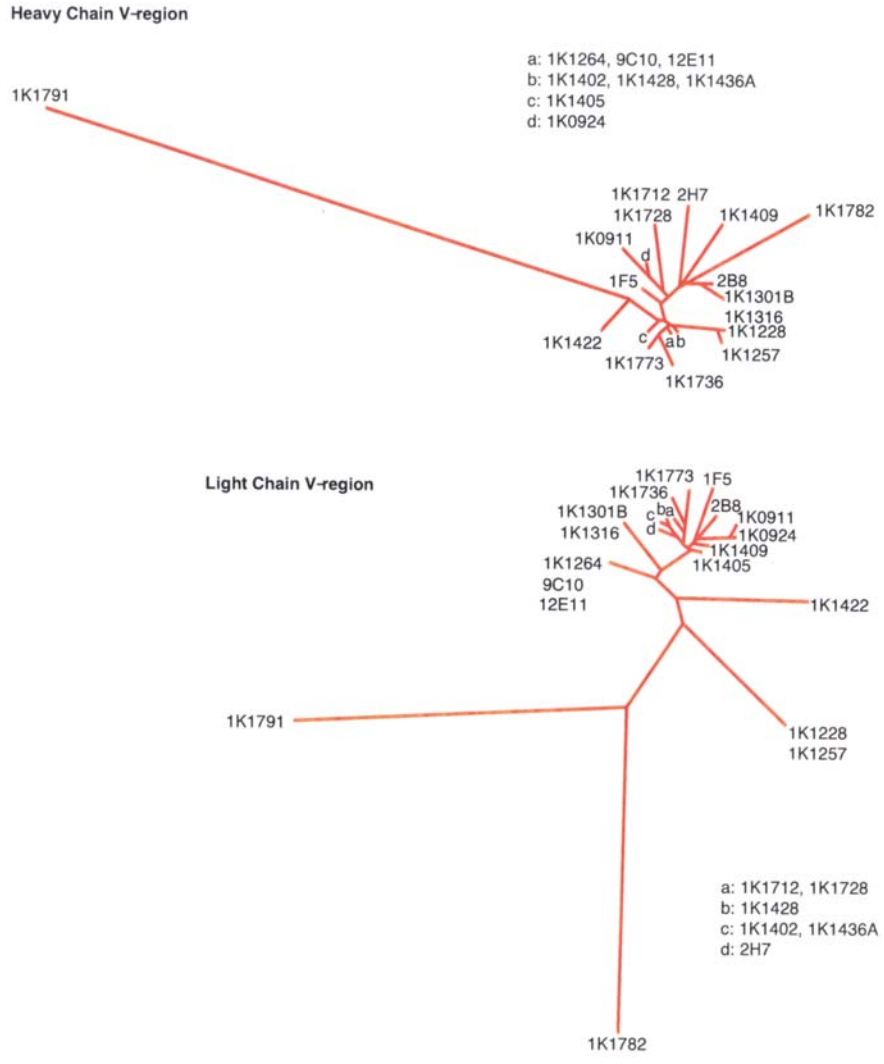

Figure 1. Phylogenetic tree analysis of amino acid sequence of anti-CD20 antibody variable regions. The relative differences of amino acid sequences of variable regions between a number of anti-CD20 mAbs and 2B8 were phylogenetically mapped employing a neighboring-joining method. Both the heavy and light chain sequences of most antibodies were very close to each other. Only the monoclonal antibody 1K1791 had a distinct heavy chain variable region and both 1K1791 and 1K1782 had light chains different from most other anti-CD20 mAbs.

added to each well of a 96-well TC plate (E&K Scientific Products, Santa Clara, CA). Raji cells [100 μl (2x10^5 cells/ml)] were added to the wells of the first row and then 100 μl serially diluted down each column. Rows were divided into those with and those without antibody. For the antibody containing wells, medium containing 10 μg/ml of both rituximab and goat anti-human IgG were added and the plate was incubated in a humidified atmosphere of 5% CO_2 at 37˚C for 24 h. Of either caspase-3/7 substrate (Promega, WI) or caspase-9 substrate (Promega), 100 μl was then added to the appropriate rows and the plates incubated on a shaker (based on the Promega technical bulletin of Caspase-Glo™ 3/7 Assay System: TB323, Caspase-Glo™ 9 Assay System). The luminescence was read after 1 and 2 h by a Wallac Victor2 plate reader (Perkin-Elmer, Waltham, MA). Duplicate control wells containing 20 μM zVAD-fmk as well as either caspase-3/7 or caspase-9 substrate and 5000 or 1250 cells, respectively, were included on the plate.

For 1K mAbs testing, Raji cells (5x10^3 cells/well) in 85 μl of medium were placed in each well of a 96-well TC flat bottom plate. Half the rows contained 10 μM zVAD-fmk and half medium alone. Of test antibody, 5 μg/ml was added to each well followed by 5 μg/ml of goat anti-murine IgG. Medium was added to all wells to bring the final volume up to 100 μl. Appropriate control wells with or without test antibody or using human IgG or murine IgG were included. Ionomycin (Calbiochem™ EMD Biosciences, San Diego, CA) in a concentration of 1 μM was used as a positive control. Cells were incubated in a humidified atmosphere of 5% CO_2 at 37˚C for 12 h and an equal volume (100 μl) of caspase-3/7 substrate was added. The plate was agitated at room temperature for 50 min and the luminescence read by a Wallac Victor2 plate reader.

Results

Characterization of novel murine anti-CD20 mAbs. Different protocols were used to generate murine mAbs directed against human CD20. Cell lines expressing CD20 or CD20-transfected CHO cells were used for priming and boosting. In addition, recombinant GST-CD20 fusion protein was used for boosting. Several mAbs were selected for further analysis and were

Table II. Mean fluorescence intensity of antibody binding to various cells.[a]

	Raji		CCRF-SB		$CD20^+$ CHO		$CD20^-$ cells	
FL1	MFI (average)	S.D.	MFI (average)	S.D.	MFI (average)	S.D.	MFI (average)	S.D.
Rituximab	$7.9x10^2$	$1.3x10^2$	$1.0x10^3$	$4.4x10^2$	$3.8x10^3$	$8.8x10^2$	1.7	0.2
1K mAbs	$6.7x10^2$	$2.1x10^2$	$7.8x10^2$	$4.3x10^2$	$3.1x10^3$	$5.8x10^2$	1.6	0.2

[a]The mean fluorescence intensity (MFI) of antibody binding to different $CD20^+$ CHO cells was determined through integration of the fluorescence histogram of each antibody as in Fig. 2. The FITC intensities detected by FL1 were averaged and compared among those of different $CD20^+$ CHO cells. Untransfected CHO DG44 or Jurkat cells were tested as negative controls. The results of the 1K mAbs were pooled to show a broad range of antibody response to cells rather than response by individual antibodies, such as rituximab.

given the nomenclature 1K followed by a number, and were then compared to murine mAbs 1F5 and 2B8, as well as the chimeric anti-human mAb c2B8 (rituximab). Eight mAbs in the 1K series were selected for examination in this study. The isotypes of the mAbs consisted of IgG1, IgG2a, and IgG2b all with a κ light chain (Table I). Affinity measurements were assessed by the use of ^{125}I-radiolabeled antibody binding to $CD20^+$ Raji cells and its displacement by different concentrations of non-radiolabeled antibodies, as described in methods. The dissociation constant (Kd) was determined for each antibody and the values are listed in Table I. There were no significant differences in the Kd values among the various 1K mAbs as well as among the other mAbs 1F5, 2B8 and c2B8. Receptor density analysis was also examined to determine the B_{max} values. As shown in Table I, the B_{max} values of all the antibodies tested ranged from $0.7\text{-}1.7x10^{-6}$. These findings demonstrate that, following the various protocols used for immunization, several novel mAbs (1K series) directed against human CD20 were generated with different isotypes. These antibodies exhibited similar Kd and B_{max} values compared to both murine 1F5 and 2B8 as well as the chimeric anti-human CD20, c2B8 (rituximab), approved by FDA. The findings with the 1K mAbs were further explored for other properties that might distinguish them from the known mAbs tested.

Analysis of amino acid sequence of both light and heavy chains of the anti-CD20 variable regions of the different 1K mAbs and the published mAbs: homologies for all except for 1K1782 and 1K1791. The variable regions of both heavy and light chains that are involved in antigen binding determine both specificity and affinity. Thus, we established the amino acid sequences of the anti-CD20 variable regions of the various 1K mAbs and determined homology as well as non-homology among these and published anti-CD20 mAbs including 2B8, 1F5 and 2H7. The data were topologically mapped by tree analysis as shown in Fig. 1. In this figure, it is noted that all 1K mAbs and the published anti-CD20 mAbs have almost identical amino acid sequences of the heavy chain-V region except 1K1791 (Fig. 1, top). Analysis of the light chain sequences revealed that all 1K mAbs share similar sequences of the κ light chain-V region except 1K1782 and 1K1791. The differences of the V regions of both 1K1782 and 1K1791 suggest that these two antibodies may exhibit different properties as compared with the remaining 1K mAbs or the published anti-CD20 mAbs. Likewise, the homology observed between the six mAbs suggests that these antibodies may exert similar functions. However, the epitope specificities of these various 1K mAbs could not be assigned based on the homology and differences in the amino acid sequence of the variable region or the heavy and light chains.

Binding of the various 1K mAbs to CD20-expressing cell lines as expressed by flow cytometry. The cell surface binding properties of the various mAbs to CD20-expressing cells were determined by flow cytometry as described in Materials and methods. Raji, CCRF-SB, and $CD20^+$ CHO cells were used as $CD20^+$ cells and CHO DG44 ($CD20^-$) or Jurkat cells were used as a negative control. Control normal murine Ig was used with the corresponding isotype to the test mAb. The cells were treated with an excess amount of antibody to bind, washed and treated with FITC-conjugated $F(ab')_2$ goat anti-mouse Ig and processed as described in Materials and methods for flow analysis. The data are represented in histograms (Fig. 2). For comparison, the 2B8 mAb staining is depicted in purple color, the isotype controls are depicted by green dotted lines. Clearly, there was no staining of the CHO DG44 and Jurkat cells demonstrating the specificity of the 1K mAbs. The histogram analyses show that all 1K mAbs stained Raji cells with similar intensity. With CCRF-SB, 1K mAbs stained the cells with higher intensity than with Raji and there were some differences such as that 1K1791 and 1K1782 showed less staining compared to 2B8 and other 1K mAbs. Analysis of the CD20-transfected CHO cells showed that all 1K mAbs stained the cells with significantly higher intensity as compared to Raji and CCRF-SB. The high intensity staining of $CD20^+$ CHO cells reflects the overexpression of cell surface CD20 compared to non-transfected Raji and CCRF-SB (Table II).

In addition to flow cytometry, the binding of the various mAbs to the $CD20^+$ CHO cells was also analyzed by ELISA, as described in Materials and methods. Different concentrations of the antibodies were used, their binding to $CD20^+$ CHO cells determined and the data were analyzed (Fig. 3). The binding was found to be dependent on the concentration of the antibody used. At a low concentration of 3 ng/ml, there was little binding of 2B8 and 1K mAbs except for 1K1712 that was relatively

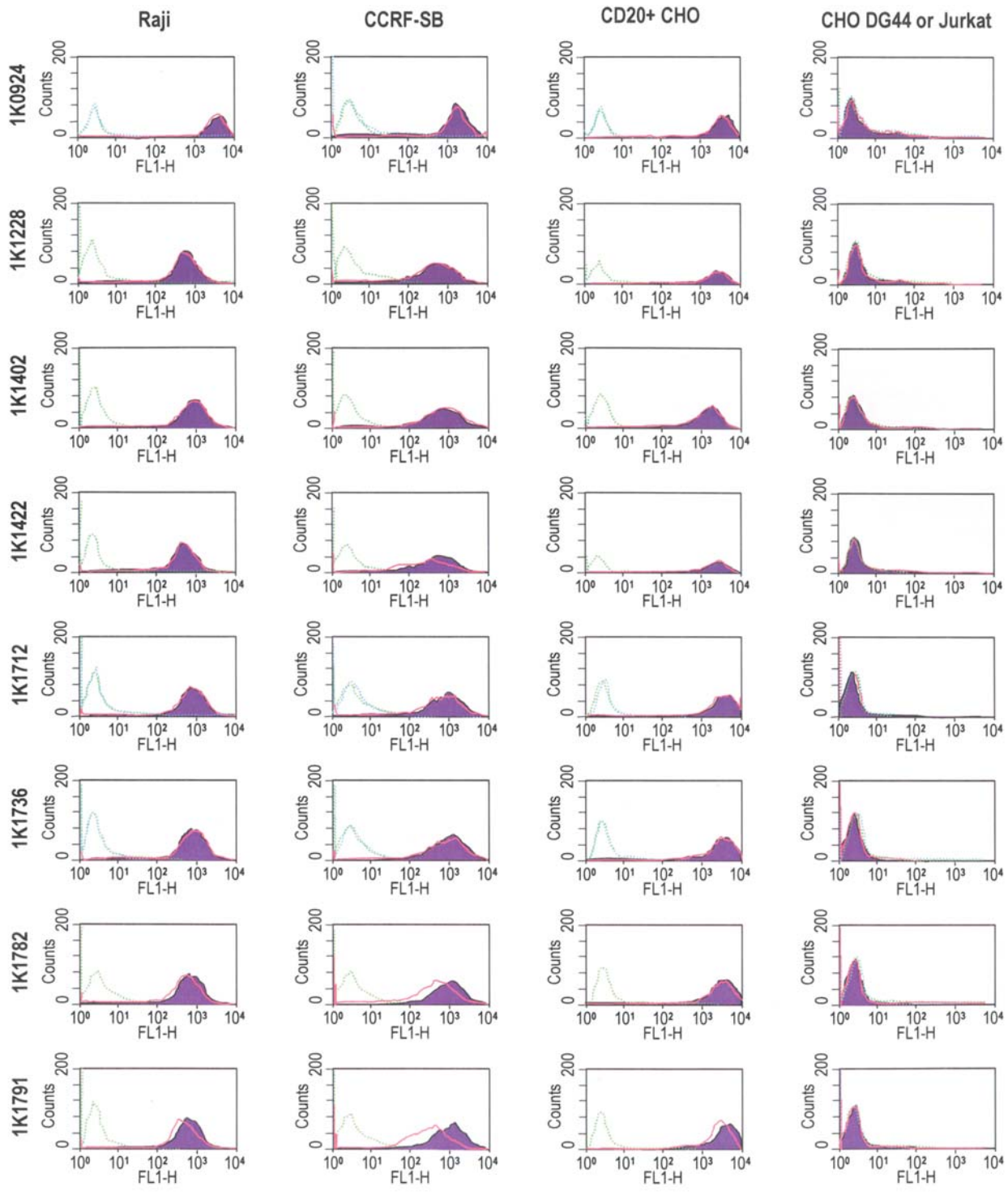

Figure 2. Flow cytometry analysis of the various monoclonal antibodies. The FITC fluorescence intensity was detected by FL1 in flow cytometry analysis. Rows 1-8 are 1K0924, 1K1228, 1K1402, 1K1422, 1K1712, 1K1736, 1K1782 and 1K1791 and columns 1-3 show the reactivity to Raji, CCRF-SB and CD20$^+$ CHO respectively. The 4th column shows binding to CHO DG44 host (CD20$^-$) (lines 1-4) and Jurkat (lines 5-8). 2B8 staining is depicted in a solid purple color as a positive control and its isotype control, IgG1, κ by green dotted line. 1K mAbs are depicted by a pink solid line and isotype control antibodies by an aqua dotted line.

higher than others. By increasing the concentration of the antibodies, there was increased binding of up to 100-316 ng/ml and a plateau was achieved. The binding by the various 1K mAbs showed some differences. For example, 1K1712 was the most efficient binder followed by 1K1736 and there was equal binding by 2B8, 1K0924, 1K1782 and 1K1402. Both 1K1791 and 1K1422 were the poorest binders. The binding was specific as control IgGs did not show any activity. These findings suggest that the various mAbs may have different activity on CD20$^+$ overexpressing cells.

Inhibition of Raji cell growth by 1K mAbs. The previous findings demonstrated the ability of various 1K mAbs to bind cell surface expression on various CD20$^+$ cell lines. We

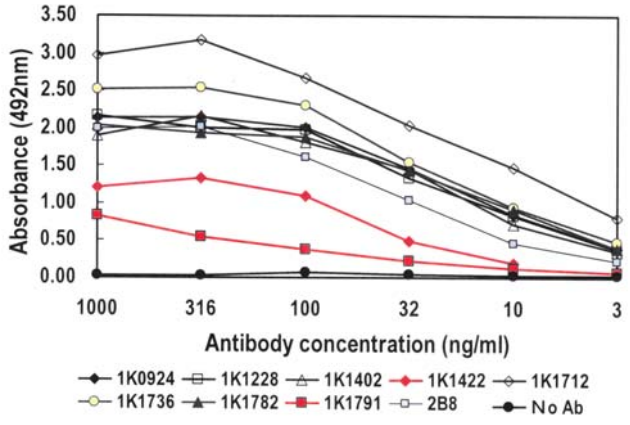

Figure 3. Analysis of antibody binding to CD20+ CHO by whole cell ELISA. Antibody reactivity to CD20+ CHO fixed on a PLL plate was tested as described in Materials and methods.

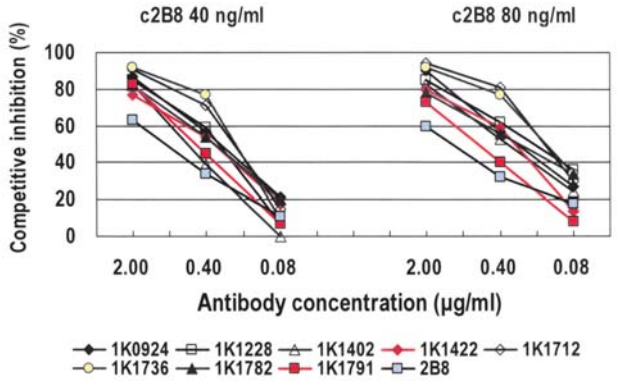

Figure 5. Competitive inhibition of binding of c2B8 on Raji by the various 1K and 2B8 monoclonal antibodies. Two concentrations of c2B8, 40 and 80 ng/ml, were used and different concentrations of 1K mAbs and 2B8 were used for competitive binding as described in Materials and methods.

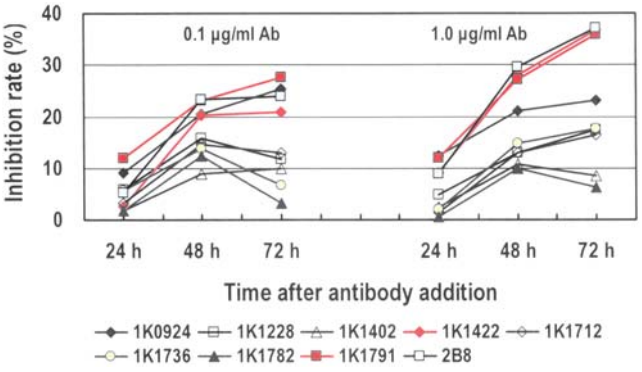

Figure 4. Inhibition of Raji cell growth by the various monoclonal antibodies. The inhibitory effects of the 1K series of mAbs and 2B8 at two different concentrations (0.1 or 1.0 μg/ml) on Raji cells were examined over 24-72 h. The percent inhibition of cell growth was determined as cell growth without mAbs (100%) minus cell growth rate (%) in the presence of mAb, where cell growth was determined by the luminescence.

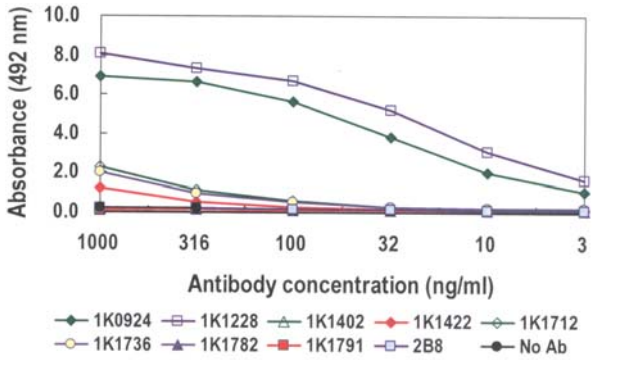

Figure 6. Binding of the various 1K mAbs and 2B8 to recombinant fixed GST-CD20. The binding of the various mAbs to GST-CD20 was performed as described in Materials and methods.

examined the effect of these antibodies on cell growth of Raji cells in culture (Fig. 4). Raji cells were treated with various concentrations of 1K mAbs and cultured for up to 72 h. The cells were harvested at different times and cell growth was determined by the luminescent method as described in Materials and methods. When 0.1 μg/ml mAb was used, there was significant inhibition of cell growth by 1K1791, 1K0924, 1K1422 and 2B8 at both 48 and 72 h of culture. The remaining antibodies did not exert any significant inhibitory effect on the growth of Raji cells. When a higher concentration of antibody was used (1.0 μg/ml), there was a more pronounced inhibition. The mAbs 1K1791, 1K1422, 2B8 and 1K0924, showed a time-dependent inhibition of cell growth, though 1K0924 showed less inhibition than the other three mAbs. Even at a higher concentration of 1.0 μg/ml, 1K1402, and 1K1782 did not result in any inhibitory activity of Raji cell growth. These findings demonstrate that three of the 1K mAbs behave like 2B8 in inhibiting Raji cell growth in a time- and concentration-dependent manner. Further, the studies demonstrate that, although the non-inhibiting 1K mAbs bind to CD20 on Raji cells with the same intensity as the three inhibitory 1K mAbs, the mere binding is not sufficient to exert an inhibitory effect of cell growth. It is possible, however, that the non-inhibitory activity on Raji cells may not be generalized to other cell lines. The findings demonstrating that three mAbs can inhibit cell growth suggest that these antibodies signal the cells through their interaction with their CD20 receptor and affect DNA replication. The inhibitory effect of cell growth shown above by the 1K mAbs did not discriminate between the cytostatic effect and cytotoxic effect and further analyses are shown below.

Epitope specificity of the 1K mAbs as assessed by competitive inhibition of binding of 2B8 to CD20+ CHO cells. 2B8 mAb was used to genetically engineer the chimeric c2B8 (rituximab) that was approved by the FDA in 1997 for the treatment of B-NHL. Thus, we examined the relationship between the epitope binding specificity of the various 1K mAbs in comparison to that of c2B8. Competitive binding was assessed by using immobilized CD20+ CHO cells on 96-well plates and the luminescent ELISA method was used as described in Materials and methods. Two concentrations of c2B8 were used, 40 and 80 ng/ml. The findings are presented in Fig. 5. At a lower concentration of 40 ng/ml of c2B8 mAb, all of the 1K mAbs and 2B8 mAb significantly competitively inhibited the binding of c2B8 on CD20+ CHO cells. The inhibition was dependent on the concentration of the antibody used; a

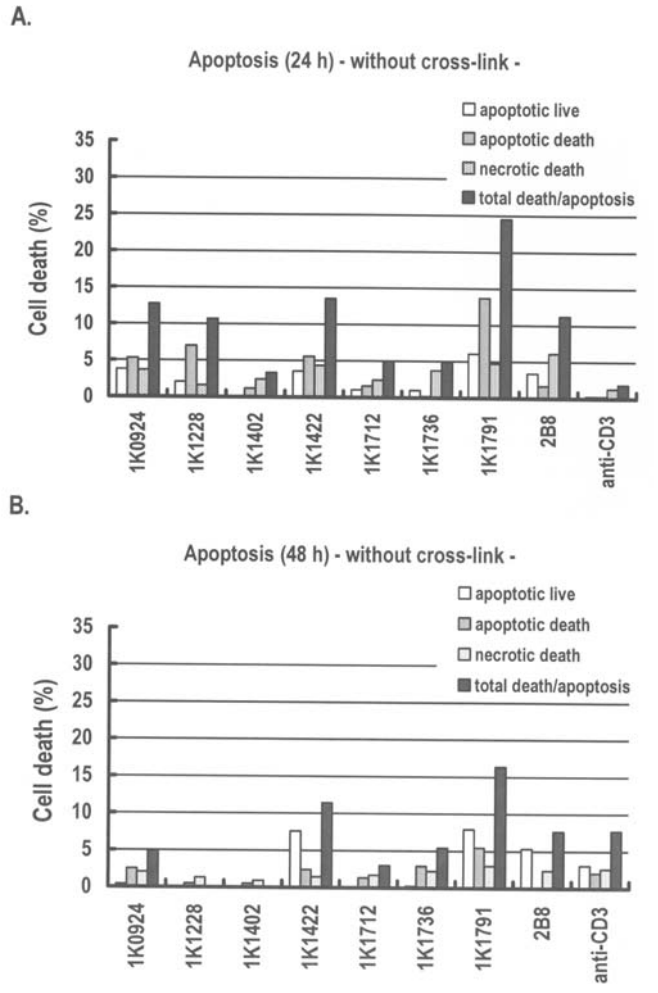

Figure 7. Analysis of cell death mediated by various mAbs on Raji cells. Raji cells were treated with the mAb for 24 h (A) and 48 h (B). 2B8 was used as a positive control and murine anti-CD3 mAb as the negative control.

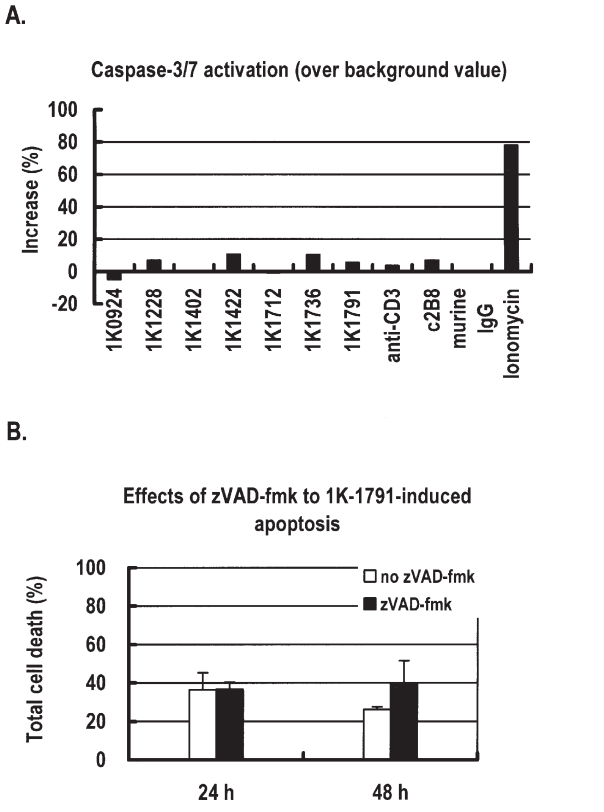

Figure 8. (A) Failure of caspase-3/7 activation by the various mAbs and (B) failure of the pan-caspase inhibitor zVAD-fmk to inhibit 1K1791-induced apoptosis of Raji cells. Caspase-3/7 substrate was used to detect the caspase-dependent apoptosis activation by various mAbs comparing to ionomycin which induces significant activation of caspase signal cascade. The effect of zVAD-fmk on 1K1791-induced apoptosis of Raji cells was tested as described in Materials and methods.

concentration of 2 μg/ml was more inhibitory than lower concentrations. All of the 1K mAbs showed similar competitive inhibition at all 3 antibody concentrations used. Interestingly, 2B8 competed less strongly than the 1K mAbs for c2B8 binding. Similar findings to those observed with a c2B8 concentration of 40 ng/ml were also found when a higher concentration of 80 ng/ml c2B8 was used.

These findings suggest that the ability of the various 1K mAbs to bind to CD20 and prevent c2B8 binding is because either the same epitope is recognized by the antibodies and/or that some of the mAbs may mask the c2B8 epitope through their binding to adjacent epitopes. The latter possibility may explain why some of the 1K mAbs fail to inhibit cell growth, while others such as c2B8 were successful.

Epitope specificity as determined by binding of the 1K mAbs to recombinant GST-CD20 fusion protein. Recombinant GST-CD20 protein was immobilized on a 96-well PLL plate and used for determining antibody binding by the luminescent ELISA assay as described in Materials and methods. Different concentrations of the 1K mAbs and 2B8 were used for binding to immobilized GST-CD20. The data represented in Fig. 6 showed that only two 1K mAbs, namely 1K0924 and 1K1228, could bind to GST-CD20 in a concentration-dependent manner, whereas the remaining 1K mAbs and 2B8 did not show any binding above control even at very high concentration of antibody. The binding was specific as control Ig isotypes did not show any detectable binding. These findings demonstrate that even though all the mAbs recognize cell surface CD20 expression on the cells, they behave differently when CD20 is not expressed on the cell surface but is in a soluble form. These results suggest that 1K0924 and 1K1228 may recognize epitopes different from the remaining 1K mAbs and that they may recognize a non-conformational epitopes expressed by the soluble GST-CD20 molecule.

Cytotoxic activity of the various 1K mAbs. The ability of the various 1K mAbs to exert a cytotoxic effect on Raji cells was examined by flow cytometry by Annexin V-FITC/PI staining method, as described in Materials and methods. This method allows the examination of live cells (Annexin$^-$/PI$^-$), early stage of apoptosis (Annexin$^+$/PI$^-$) and late-stage apoptosis (Annexin$^+$/PI$^+$) and necrotic cells (Annexin$^-$/PI$^+$). Raji cells were treated with optimal concentration of mAbs for 24 and 48 h and analyzed for cell death as described above. The findings are summarized in Fig. 7A and B. Clearly, all of the antibodies tested had minimal cytotoxic effect on Raji cells except for 1K1791. 2B8 also did not demonstrate such cytotoxicity as reported previously (34,35). There was minimal necrotic cell death by the antibodies. Examination of apoptosis revealed that

Table III. Comparison of properties of anti-CD20 mAbs.

Properties	2B8 IgG1, κ	1K0924 IgG2b, κ	1K1228 IgG1, κ	1K1402 IgG1, κ	1K1422 IgG1, κ	1K1712 IgG2a, κ	1K1736 IgG2b, κ	1K1782 IgG1, κ	1K1791 IgG1, κ
Physical and immunological									
Binding affinity (Kd)	1.26 nM[a]	2.23 nM	1.26 nM	1.25 nM	2.07 nM	1.70 nM	1.24 nM	NT	3.61 nM
Maximum binding (B_{max})	$1.3x10^{5a}$	$6.7x10^4$	$1.6x10^5$	$1.7x10^5$	$1.3x10^5$	$7.4x10^4$	$1.7x10^5$	NT	$1.5x10^5$
MFI to Raji cells ($x10^2$)	7.9	5.0	6.2	9.8	5.3	8.4	9.2	5.1	4.8
to CCRF-SB cells ($x10^2$)	10.0	17.0	6.0	6.5	5.0	8.9	10.0	5.8	3.2
to $CD20^+$ CHO cells ($x10^2$)	38.0	30.0	29.0	20.0	32.0	40.0	36.0	32.0	30.0
Reactivity to GST-CD20	-	+++++	+++++	-	+	++	++	-	-
Reactivity to $CD20^+$ CHO	+++	++++	+++	+++	++	+++++	++++	+++	+
Binding competition with 2B8	++	+++	++++	+++	+++	+++++	+++++	+++	+++
Difference of MFI from 2B8	-	-	-	-	+	-	-	++	++
H-chain AA seq. correlation to 2B8	0	+	+	+	+	+	++	++	+++++
L-chain AA seq. correlation to 2B8	0	+	++	+	++	+	+	+++++	+++++
Biological									
Direct inhibition of cell growth	+++	++	±	±	++	+	+	±	++++
Apoptosis at 24 h (Raji cells)	+	+	+	-	+	-	-	NT	+++
Apoptosis at 48 h (Raji cells)	+	-	-	-	++	-	-	NT	++
Caspase-3/7 activation	-	-	-	-	-	-	-	-	-

Binding affinity was determined by Scatchard analysis. The MFIs described in this table are original data of Table II. Reactivity to GST-CD20 was measured by ELISA. Reactivity to $CD20^+$ CHO cells and binding competition with 2B8 were measured by whole cell ELISA. Amino acid sequence (AA seq.) correlation was demonstrated by relative distance from that of rituximab based on phylogenetic trees. Apoptosis includes apoptotic death and apoptotic life without cross linker. Reactivity ranged from + through a maximum of +++++ with - for negative and ± when it was not clear. [a]c2B8 (rituximab) was used instead of 2B8. NT, not tested; H-chain, heavy-chain; L-chain, light-chain.

all of the mAbs tested were negative except 1K1791 which induced reproducible apoptosis on Raji cells. Noteworthy, 1K1971 also showed significant inhibition of Raji cell growth as shown in Fig. 4. However, 2B8, 1K1422 and 1K0924 were non-apoptotic, although they demonstrated significant inhibition of cell growth. While the various 1K mAbs did not induce apoptosis, it is possible that the use of a secondary IgG antibody to mouse IgG may induce cross-linking and may result in apoptosis. This will be the subject of a separate study.

Apoptosis induction by 1K1791 is caspase-independent. The induction of apoptosis by various stimuli is believed to proceed through the activation of the extrinsic death receptor pathway (Type I) or by the intrinsic mitochondrial pathway (Type II). Both of these pathways induce apoptosis through the activation of effector and executioner caspases. However, there are also reports of the induction of apoptosis which is independent of caspase activation (16,36,37). We, therefore, investigated the mechanism by which anti-CD20 mAbs induce apoptosis in Raji cells. We first examined the activation of caspase-3 and -7 as described in Materials and methods. The calcium ionophore, ionomycin, is a strong inducer of apoptosis and was used as a positive control for caspase activation. None of the 1K mAbs activated caspase-3 and -7, including 1K1791 as shown in Fig. 8A. By contrast, ionomycin significantly activated both of these caspases. Based on the lack of activation of caspase-3 and -7 by 1K1791, we further examined the effect of the pan-caspase inhibitor, zVAD-fmk, as apoptosis inhibitor. The effect of this inhibitor on 1K1791-induced apoptosis of Raji cells was tested at both 24 and 48 h. Clearly, the apoptosis induced by 1K1791 was not inhibited by zVAD-fmk when examined at both 24 and 48 h of treatment (Fig. 8B). These findings suggest that 1K1791 can induce apoptosis independently of caspase activation.

Properties of the novel anti-CD20 mAbs (1K series) and their comparison to 2B8. The above studies examined several properties of the novel 1K series anti-human CD20 mAbs and compared their properties to the well-known 2B8 antibody. The findings are summarized in Table III. Clearly, distinct differences were observed with the various mAbs tested. Based on the limited analyses performed thus far, 1K1791 appears to be superior even to 2B8 in its ability to inhibit cell growth and induces caspase-independent apoptosis in the absence of secondary cross-linking. The 1K1791 mAb also showed significant difference in amino acid sequence of both heavy and light chains compared to other antibodies. In addition, 1K1782 also has a different sequence and it will be important to test its apoptotic activity (1K1782 was not tested due to the limited quantity of antibody available).

Discussion

The present study characterized eight novel murine 1K mAbs directed against human CD20 and compared their properties to 2B8 or c2B8. All of the mAbs used at saturating concentrations reacted with CD20-expressing cell lines with intensity similar to 2B8 or c2B8. However, titration of the Abs and their binding to CD20-transfected CHO ($CD20^+$ CHO) cells revealed significant differences in their binding intensity. For instance, 1K1712 and 1K1736 showed superior binding activity compared to the other 1K mAbs and 2B8. 1K1791 mAb showed the poorest binding intensity. Three 1K mAbs (1K1791, 1K0924, 1K1422) showed similar ability to inhibit cell growth compared to 2B8. While all 1K mAbs competitively inhibited the binding of c2B8 to $CD20^+$ cells, only 1K1228 and 1K0924 were found to bind fixed recombinant GST-CD20. Like c2B8 and 2B8, none of the 1K mAbs induced apoptosis in Raji cells except 1K1791, and the apoptosis induced by 1K1791 was caspase-independent. These findings show that some novel murine anti-human mAbs exhibit properties different from 2B8 and c2B8, and suggest that such antibodies may also exhibit different activities on B-NHL when compared to 1F5, 2B8, or c2B8. These novel mAbs, therefore, justify further preclinical development to examine their effectiveness compared to currently available CD20 mAbs.

All of the eight 1K mAbs bind cell surface CD20 on several CD20-expressing cell lines as well as $CD20^+$ CHO cells. The binding at saturating concentration was comparable to 2B8. However, when the antibodies were titrated for binding to $CD20^+$ CHO, significant differences were observed in the binding intensity and antibody concentration required to reach plateau. Two 1K mAbs, 1K1712 and 1K1736, showed significantly higher binding intensity compared to all other 1K mAbs and 2B8. Nine-fold lower concentration of 1K1712 was required to achieve the same binding intensity as other antibodies. The 1K1422 and 1K1791 mAbs were weak binders to $CD20^+$ CHO cells. These findings suggest that the high binding 1K1712 and 1K1736 may have different biological and anti-tumor activity compared to 2B8 and other 1K mAbs. Further, these two antibodies may trigger the cell and interfere with intracellular signaling pathways, as has been shown with rituximab (6).

Analysis of the ability of the 1K mAbs to inhibit cell growth revealed that the inhibition of Raji cell growth by three of the 1K mAbs (1K0924, 1K1791, and 1K1422) was comparable to 2B8-induced inhibition. In comparison with the ability of the 1K mAbs to bind CD20, and also the distinctive superiority of 1K1712 and 1K1736 in binding $CD20^+$ CHO cells, there does not seem to be a correlation between the ability of a particular 1K mAb to bind CD20 and its ability to inhibit cell growth. The mechanism responsible for the inhibition of cell growth is not known. It has been reported that 2B8 and c2B8 inhibit cell growth by cytostasis and not by induction of cell death by apoptosis. Among the three 1K mAbs shown to inhibit cell growth, only 1K1791 mAb was shown to induce meaningful apoptosis. Thus the apoptosis induced by 1K1791 might have contributed to its effect in inhibiting cell growth. The fact that three 1K mAbs inhibited cell growth suggested that these antibodies might have delivered signals which interfered with gene products responsible for cell growth and proliferation.

Studies were performed to determine the epitope specificity of the 1K mAbs by two methods. The first method examined the ability of the 1K mAbs to compete for binding of rituximab to $CD20^+$ CHO cells. Interestingly, all of the eight 1K mAbs competed equally for rituximab binding, suggesting that either the 1K antibodies recognize similar or adjacent epitope similar to the epitope recognized by rituximab or that the 1K mAb antibodies may sterically interfere with rituximab binding. In order to further define the epitope specificities of the 1K mAbs, further studies using epitope mapping (26,27) or mutation of critical amino acid residues involved in rituximab binding (20,26,27) will be required. A second method was used to define epitope specificities and involved the binding of the 1K mAbs to an extracellular CD20 molecule in the form of fixed GST-CD20 fusion protein. Noteworthy, two mAbs 1K0924 and 1K1228 were found to bind GST-CD20, while the remaining 6 mAbs and 2B8 showed no binding comparable to Ig control. These findings are significant in that the antibodies that bound native CD20 but did not bind to the fusion protein probably recognized conformational epitopes. This, however, needs to be addressed by the use of overlapping peptides as recently reported by Teeling *et al* (27). These authors reported for the first time that the human CD20 antibodies tested recognized a region in the small loop of CD20 whereas other CD20 mAbs tested did not bind to the small loop but all bound to the large loop of CD20. Hence, it is possible that 1K0924 and 1K1228 may also recognize the small loop of CD20 and further studies are therefore needed to address this possibility.

By examining the ability of 1K mAbs to induce cell death in Raji, it was found that only 1K1791 could induce modest but significant apoptosis in Raji cells. All other 1K mAbs and 2B8 were not cytotoxic or apoptotic, although their effect on other CD20-expressing cell lines awaits further investigation. The ability of 1K1791 to induce apoptosis is a unique feature of some 1K mAbs. For instance, Cardarelli *et al* (28), as later confirmed by Cragg and Glennie (29) demonstrated that the murine B1 anti-CD20 mAb and $F(ab')_2$ could induce direct apoptosis of B cell lines in the absence of secondary cross-linking with anti-IgG. It is not clear what determines the ability of an anti-CD20 antibody to induce apoptosis while others do not. It has been suggested that the apoptosis-inducing antibodies compared to non-apoptosis-inducing antibodies have the ability to bind at a half maximal level of saturation (16,29). Rituximab has been shown to induce apoptosis following hyper-cross-linking (30-32). Thus, the 1K mAbs may have the ability to induce apoptosis following hyper-cross-linking and such issues are under current investigation. The role of CD20-induced direct apoptosis *in vivo* and its involvement in anti-tumor activity is not clear. Byrd *et al* (10) reported that treatment with rituximab *in vivo* induces apoptosis. However, the induction of apoptosis was not shown to be due to direct effect and an additional antibody crossing by FcR *in vivo* or through complement-dependent cytotoxicity has not been ruled out (33). The apoptosis induced by 1K1791 was also found to be caspase-independent. These findings are consistent with the findings of Chan *et al* (16) for other anti-CD20 antibodies. It is notable that many of the antibodies showed

similar variable sequences to 2B8 and some were markedly different, e.g. 1K1791 and 1K1782. Whether these dissimilar sequences reflected the selection of different variable region genes and whether there is a correlation with the selection of a particular gene family and biological function is beyond the scope of this study. Although relationships between specific variable region gene families and antigen specificity have been noted in other systems as reported by Li *et al* (38), it would be interesting to know whether a directed selection of a specific variable region gene or elimination of others would lead to the development of antibodies with more varied or unusual biological characteristics.

In summary, the present findings identified novel CD20 mAbs that exhibit properties that are different from 2B8 and rituximab. Further studies are necessary to examine the therapeutic efficacy *in vivo* with tumor xenografts and also investigate the underlying molecular signaling induced by these antibodies and establish the ability for sensitizing resistant tumor cells to both chemotherapy and immunotherapy. Further, studies with $F(ab')_2$ fragments may provide additional information on the direct role of apoptosis *in vivo* in tumor regression. Most important is the evaluation of the 1K mAbs for their ability to have an effect on rituximab-resistant tumor cells.

Acknowledgments

The authors acknowledge Doctor Benjamin Bonavida for assisting in the revision and advising in the preparation of this manuscript. Also, we acknowledge the administrative assistance of Alina Katsman, Maggie Yang and Zenyaku Kogyo for generously providing mAbs for our study.

References

1. Reff ME, Carner K, Chambers KS, *et al*: Depletion of B cells *in vivo* by a chimeric mouse human monoclonal antibody to CD20. Blood 83: 435-445, 1994.
2. Stern M and Herrmann R: Overview of monoclonal antibodies in cancer therapy: present and promise. Crit Rev Oncol Hematol 54: 11-29, 2005.
3. Tedder TF and Engel P: CD20: a regulator of cell-cycle progression of B lymphocytes. Immunol Today 15: 450-454, 1994.
4. Liang Y, Buckley TR, Tu L, Langdon SD and Tedder TF: Structural organization of the human MS4A gene cluster on Chromosome 11q12. Immunogenetics 53: 357-368, 2001.
5. Cragg MS, Walshe CA, Ivanov AO and Glennie MJ: The biology of CD20 and its potential as a target for mAb therapy. Curr Dir Autoimmun 8: 140-174, 2005.
6. Jazirehi AR and Bonavida B: Cellular and molecular signal transduction pathways modulated by rituximab (rituxan, anti-CD20 mAb) in non-Hodgkin's lymphoma: implications in chemosensitization and therapeutic intervention. Oncogene 24: 2121-2143, 2005.
7. Glennie MJ and Johnson PW: Clinical trials of antibody therapy. Immunol Today 21: 403-410, 2000.
8. Coiffier B: Monoclonal antibodies in the management of newly diagnosed, aggressive B-cell lymphoma. Curr Hematol Rep 2: 23-29, 2003.
9. Bannerji R, Kitada S, Flinn IW, Pearson M, Young D, Reed JC and Byrd JC: Apoptotic-regulatory and complement-protecting protein expression in chronic lymphocytic leukemia: relationship to *in vivo* rituximab resistance. J Clin Oncol 21: 1466-1471, 2003.
10. Byrd JC, Kitada S, Flinn IW, Aron JL, Pearson M, Lucas D and Reed JC: The mechanism of tumor cell clearance by rituximab *in vivo* in patients with B-cell chronic lymphocytic leukemia: evidence of caspase activation and apoptosis induction. Blood 99: 1038-1043, 2002.
11. Dyer MJ, Hale G, Hayhoe FG and Waldmann H: Effects of CAMPATH-1 antibodies *in vivo* in patients with lymphoid malignancies: influence of antibody isotype. Blood 73: 1431-1439, 1989.
12. Weng WK and Levy R: Expression of complement inhibitors CD46, CD55, and CD59 on tumor cells does not predict clinical outcome after rituximab treatment in follicular non-Hodgkin lymphoma. Blood 98: 1352-1357, 2001.
13. Isaacs JD, Greenwood J and Waldmann H: Therapy with monoclonal antibodies. II. The contribution of Fc gamma receptor binding and the influence of C(H)1 and C(H)3 domains on *in vivo* effector function. J Immunol 161: 3862-3869, 1998.
14. Manches O, Lui G, Chaperot L, *et al*: *In vitro* mechanisms of action of rituximab on primary non-Hodgkin lymphomas. Blood 101: 949-954, 2003.
15. Cragg MS, Morgan SM, Chan HT, *et al*: Complement-mediated lysis by anti-CD20 mAb correlates with segregation into lipid rafts. Blood 101: 1045-1052, 2003.
16. Chan HT, Hughes D, French RR, *et al*: CD20-induced lymphoma cell death is independent of both caspases and its redistribution into triton X-100 insoluble membrane rafts. Cancer Res 63: 5480-5489, 2003.
17. Cheson BD: Monoclonal antibody therapy of chronic lymphocytic leukemia. Cancer Immunol Immunother 55: 188-196, 2006.
18. Summers KM and Kockler DR: Rituximab treatment of refractory rheumatoid arthritis. Ann Pharmacother 39: 2091-2095, 2005.
19. Polyak MJ, Tailor SH and Deans JP: Identification of a cytoplasmic region of CD20 required for its redistribution to a detergent-insoluble membrane compartment. J Immunol 161: 3242-3248, 1998.
20. Polyak MJ and Deans JP: Alanine-170 and proline-172 are critical determinants for extracellular CD20 epitopes; heterogeneity in the fine specificity of CD20 monoclonal antibodies is defined by additional requirements imposed by both amino acid sequence and quaternary structure. Blood 99: 3256-3262, 2002.
21. Perosa F, Favoino E, Caragnano MA and Dammacco F: Generation of biologically active linear and cyclic peptides has revealed a unique fine specificity of rituximab and its possible cross-reactivity with acid sphingomyelinase-like phosphodiesterase 3b precursor. Blood 107: 1070-1077, 2006.
22. Urlaub G, Mitchell PJ, Kas E, Chasin LA, Funanage VL, Myoda TT and Hamlin J: Effect of gamma rays at the dihydrofolate reductase locus: deletions and inversions. Somat Cell Mol Genet 12: 555-566, 1986.
23. Frorath B, Abney CC, Berthold H, Scanarini M and Northemann W: Production of recombinant rat interleukin-6 in Escherichia coli using a novel highly efficient expression vector pGEX-3T. Biotechniques 12: 558-563, 1992.
24. Lindmo T, Boven E, Cuttitta F, Fedorko J and Bunn PA Jr: Determination of the immunoreactive fraction of radiolabeled monoclonal antibodies by linear extrapolation to binding at infinite antigen excess. J Immunol Methods 72: 77-89, 1984.
25. Saitou N and Nei M: The neighbor-joining method: a new method for reconstructing phylogenetic trees. Mol Biol Evol 4: 406-425, 1987.
26. Teeling JL, French RR, Cragg MS, *et al*: Characterization of new human CD20 monoclonal antibodies with potent cytolytic activity against non-Hodgkin lymphomas. Blood 104: 1793-1800, 2004.
27. Teeling JL, Mackus WJ, Wiegman LJ, *et al*: The biological activity of human CD20 monoclonal antibodies is linked to unique epitopes on CD20. J Immunol 177: 362-371, 2006.
28. Cardarelli PM, Quinn M, Buckman D, *et al*: Binding to CD20 by anti-B1 antibody or F(ab')(2) is sufficient for induction of apoptosis in B-cell lines. Cancer Immunol Immunother 51: 15-24, 2002.
29. Cragg MS and Glennie MJ: Antibody specificity controls *in vivo* effector mechanisms of anti-CD20 reagents. Blood 103: 2738-2743, 2004.
30. Shan D, Ledbetter JA and Press OW: Signaling events involved in anti-CD20-induced apoptosis of malignant human B cells. Cancer Immunol Immunother 48: 673-683, 2000.
31. Jazirehi AR, Vega MI, Chatterjee D, Goodglick L and Bonavida B: Inhibition of the Raf-MEK1/2-ERK1/2 signaling pathway, Bcl-xL down-regulation, and chemosensitization of non-Hodgkin's lymphoma B cells by Rituximab. Cancer Res 64: 7117-7126, 2004.

32. Jazirehi AR, Huerta-Yepez S, Cheng G and Bonavida B: Rituximab (chimeric anti-CD20 monoclonal antibody) inhibits the constitutive nuclear factor-{kappa}B signaling pathway in non-Hodgkin's lymphoma B-cell lines: role in sensitization to chemotherapeutic drug-induced apoptosis. Cancer Res 65: 264-276, 2005.
33. Nauta AJ, Daha MR, Tijsma O, van de Water B, Tedesco F and Roos A: The membrane attack complex of complement induces caspase activation and apoptosis. Eur J Immunol 32: 783-792, 2002.
34. Ghetie MA, Bright H and Vitetta ES: Homodimers but not monomers of Rituxan (chimeric anti-CD20) induce apoptosis in human B-lymphoma cells and synergize with a chemotherapeutic agent and an immunotoxin. Blood 97: 1392-1398, 2001.
35. Pedersen IM, Buhl AM, Klausen P, Geisler CH and Jurlander J: The chimeric anti-CD20 antibody rituximab induces apoptosis in B-cell chronic lymphocytic leukemia cells through a p38 mitogen activated protein-kinase-dependent mechanism. Blood 99: 1314-1319, 2002.
36. Stanglmaier M, Reis S and Hallek M: Rituximab and alemtuzumab induce a nonclassic, caspase-independent apoptotic pathway in B-lymphoid cell lines and in chronic lymphocytic leukemia cells. Ann Hematol 83: 634-645, 2004.
37. Daniels I, Abulayha AM, Thomson BJ and Haynes AP: Caspase-independent killing of Burkitt lymphoma cell lines by rituximab. Apoptosis 11: 1013-1023, 2006.
38. Li Y, Spellerberg MB, Stevenson FK, Capra JD and Potter KN: The I binding specificity of human VH4-34 (VH4-21) encoded antibodies is determined by both VH framework region 1 and complementarity determining region 3. J Mol Biol 256: 577-589, 1996.